JOURNAL OF GUIDANCE, CONTROL, AND DYNAMICS
Vol. 31, No. 4, July–August 2008

Low-Thrust Nonlinear Guidance by Tracking Mean Orbital Elements

Yang Gao*
Chinese Academy of Sciences, 100080 Beijing, People's Republic of China

DOI: 10.2514/1.31256

A low-thrust nonlinear guidance for long-duration, many-revolution transfer trajectories is constructed by tracking mean orbital elements based on the concept of semi-analytic satellite theory. Three simple control laws are applied over appropriate orbital arc segments within each transfer revolution to simultaneously change semimajor axis, eccentricity, and inclination. The analytic time rates of mean classical orbital elements using the proposed control strategy are computed by an orbital averaging method. Along the mean elements of nominal transfer trajectories, a tracking guidance scheme is developed using the concept of nonlinear model predictive control over finite time horizons, in which simple constrained optimization problems are formed to minimize mean orbital elements errors between the actual and nominal trajectories. Rosenbrock's optimization method, which does not calculate derivatives, guarantees robustness for optimum searching with a small number of parameters. The approach for removing deviations from the nominal trajectories is based on the changeable powered arc lengths of different steering programs and the mechanism of variable specific impulse modulation. Furthermore, the Earth's oblateness and shadow effects are taken into consideration in the guidance scheme.

Introduction

LOW-THRUST propulsion, such as solar electric propulsion (SEP), is a promising option for spacecraft to transfer between different orbits in near-Earth space. However, designing optimal Earth-orbit transfer trajectories using SEP as the primary means of propulsion still poses challenges because low-thrust acceleration is much lower than gravitational acceleration. Earth-orbit transfer trajectories, unlike interplanetary transfer trajectories, usually consist of hundreds or even thousands of orbital revolutions due to low thrust-to-weight ratios which are usually on the order of 10^{-5}. A number of methods have been developed in the past decade to solve long-duration, many-revolution transfers considering certain realistic perturbations [1–5]. These studies revealed potential uses of low-thrust propulsion for future near-Earth missions from the theoretical point of view. Recently, the SMART-1 spacecraft [6] demonstrated the practical operation of SEP to perform a successful Earth–moon orbital transfer, part of which is in near-Earth space.

A spacecraft can fly along a reference trajectory with an open-loop control designed optimally a priori. However, it may deviate from the designed optimal trajectory due to many unpredictable perturbations. Thus, an autonomous guidance scheme might become a key problem for long-duration, many-revolution, low-thrust missions. One of the most common guidance schemes is the recomputation of the optimal trajectory and control, which are uplinked to the spacecraft at certain time intervals. This scheme obviously requires plenty of offline recomputations and numerous communications between the ground station and the spacecraft, especially for long-duration Earth-orbit transfers. Furthermore, it requires a huge amount of onboard storage capacity for storing the optimal control and trajectory over time horizons that may last several months. Therefore, the scheme of recomputing and uplinking does not seem to be a preferred choice for low-thrust, long-duration transfers. In [7], based on practical flight experiences, the SMART-1 mission also suggested an autonomous guidance to reduce the operation loads from the ground. Recently, studies have been conducted on autonomous guidance for the SMART-1 and BepiColombo missions [8].

Kluever developed several guidance schemes for Earth-orbit transfers: simple open-loop guidance using blended control law [9], trajectory tracking guidance using an inverse dynamics approach [10], and trajectory tracking guidance using an empirical control law [11]. These guidance schemes, however, are only limited to cases of minimum-time transfers. Another category of low-thrust guidance is based on Lyapunov control [12–15]. Lyapunov control possesses simple form but the optimality poses a further problem. In addition, Lyapunov control in [12–15] does not consider realistic perturbations and the Earth's shadowing condition. Recently, nonlinear model predictive control has also been investigated for guidance of low-thrust spacecraft [16]. In this paper, we proposed a nonlinear guidance scheme to track the mean orbital elements of transfer trajectories, considering a coasting mechanism for fuel saving, the Earth's oblateness perturbations, and the Earth's shadowing. Meanwhile, the proposed guidance is robust even with relatively large initial orbital errors.

The concept of mean orbital elements is described in the semi-analytic satellite theory (SST) [17,18], which develops an efficient method for long-term prediction of satellite's orbits. SST computes the mean elements at large integration steps for quick trajectory propagation and recovers short-periodic terms at prescribed time constants. Therefore, SST possesses advantages in both computation speed and solution accuracy. Inspired by SST, the low-thrust transfer trajectories can also be divided into mean elements and short-periodic terms. In this paper, only the mean elements are concerned because we focused our attention on orbital transfer, not orbital prediction for which computing short-periodic terms is a must. Therefore, tracking mean elements means that it is not necessary to track any reference trajectories within a transfer revolution.

The approach presented in this paper integrates several concepts and is structured as follows. First, we reviewed the mean orbital elements derived from SST, and then included the low-thrust acceleration in time rate equations of mean elements. We then proposed a novel control strategy (presented in [5]) for guidance and developed the analytic time rates of mean elements using the control strategy. The method of trajectory optimization is briefly described to generate nominal trajectories, which are specifically suitable for the proposed guidance scheme. In terms of the nominal trajectory and control parameters, we formulated nonlinear model predictive controls over a series of finite time horizons, in which simple nonlinear constrained optimization problems are formulated. At the

Received 27 March 2007; revision received 5 December 2007; accepted for publication 22 January 2008.

*Associate Research Fellow, Academy of Opto-Electronics, Department of Space System Engineering, P.O. Box 8701; GaoY@aoe.ac.cn.

initial instant of each time horizon, an optimal open-loop control is obtained by minimizing the mean orbital element errors between the predictive and nominal trajectories at the terminal constant of the corresponding time horizon. The nonlinear constrained optimization problems are solved using Rosenbrock's method, which does not calculate derivatives and guarantees the algorithm's robustness. A series of open-loop controls over finite horizons formed a closed-loop control over the entire time span. Finally, we presented numerical examples of guidance cases for Earth-orbit transfers using SEP with constant and variable specific impulses.

This paper is an extension of the work in [5], in which trajectory optimization and open-loop guidance schemes were presented. The main contribution of this work is a robust, closed-loop, low-thrust guidance scheme for Earth-orbit transfers, employing simple trajectory control laws, a coasting mechanism for fuel saving, the timing of the powered arcs, as well as specific impulse modulation. The guidance scheme is implemented by nonlinear model predictive control, which is performed onboard to track the mean orbital elements of nominal trajectories. In addition, the Earth's oblateness and shadowing condition have been considered in this study.

Review of Semi-Analytic Satellite Theory

The semi-analytic satellite theory [17,18] proposes a method for long-term orbit prediction including all significant perturbations. The key concept of this theory is that the osculating orbital elements can be divided into mean elements and short-periodic terms with 2π period in a fast angular variable. In this work, low thrust is identified as a controllable perturbation and thereby distinguished from the original theory. Therefore, we can express the osculating elements by

$$x_i = \bar{x}_i + \eta(x_i, \mathbf{a}_T, t) \tag{1}$$

where $x_i = \begin{bmatrix} a & e & i & \Omega & \omega \end{bmatrix}$ are osculating classical orbital elements, $\bar{x}_i = \begin{bmatrix} \bar{a} & \bar{e} & \bar{i} & \bar{\Omega} & \bar{\omega} \end{bmatrix}$ are mean elements, and $\eta(x_i, \mathbf{a}_T, t)$ are short-periodic terms with the inclusion of low-thrust acceleration $\mathbf{a}_T$ and explicit time t. Note that the osculating elements can be other sets of orbital elements such as equinoctial elements used in [18]. Compared with the original SST, the low-thrust acceleration $\mathbf{a}_T$ is the key extension and thus plays a significant role during orbital transfers.

The general dynamics of the osculating and mean elements are governed by

$$\frac{\mathrm{d}x_i}{\mathrm{d}t} = f_i(a, e, i, \Omega, \omega, \mathbf{a}_T, t) \tag{2}$$

$$\frac{\mathrm{d}\bar{x}_i}{\mathrm{d}t} = A_i(\bar{a}, \bar{e}, \bar{i}, \bar{\Omega}, \bar{\omega}, \mathbf{a}_T, t) \tag{3}$$

The first-order time rates of the mean elements can be computed using an orbital averaging method. The mean elements of the transfer trajectories demonstrate a long-term characteristic, which is important for the long-duration orbital transfer problems. Therefore, it is not necessary to compute the short-periodic terms $\eta(x_i, \mathbf{a}_T, t)$, which reflect only local dynamics of orbital elements within each transfer revolution. In the following sections, we will focus our attention on constructing proper acceleration $\mathbf{a}_T$ (or control strategy), obtaining the analytic first-order time rates of mean elements with the low-thrust acceleration $\mathbf{a}_T$, and then developing the guidance scheme by tracking mean elements.

Control Strategy for Guidance

The control strategy consists of three control laws: tangential steering, inertial steering, and piecewise constant yaw steering, which are used to simultaneously change the semimajor axis, eccentricity, and inclination, respectively. These three control laws were studied separately by many researchers in the past and were originally employed by Gao [5] over different orbital arc segments. The illustration of the proposed control laws is demonstrated in Fig. 1. Within each orbital transfer revolution, the perigee-centered tangential steering is either along or opposite to velocity direction, which is the most efficient strategy to change the semimajor axis instantaneously. The apogee-centered inertial steering is perpendicular to the line of apsides, which provides a near-optimal strategy to change eccentricity. Note that the inertial steering (approximately inertial within each revolution) is not absolutely inertial in space because the line of apsides rotates slowly due to low thrust and perturbations. The piecewise constant yaw steering (perpendicular to the orbit plane) is developed to change inclination at the locations that are chosen optimally.

The tangential perigee-centered burn arc is used from s_1 to s_2, which are in turn represented by a single parameter w_s

$$s_1 = -|w_s|\pi, \qquad s_2 = |w_s|\pi \tag{4}$$

where $-1 \le w_s \le 1$. Furthermore, we define that the semimajor axis increases as $0 \le w_s \le 1$, and decreases as $-1 \le w_s < 0$. For the inertial steering, the pitch steering angle can be expressed as $\alpha = \theta$ (θ is true anomaly) to increase eccentricity. The starting and ending points (e_1 and e_2) are represented by a single parameter w_e

$$e_1 = \pi - |w_e|\pi, \qquad e_2 = \pi + |w_e|\pi \tag{5}$$

where $-1 \le w_e \le 1$. We define that the eccentricity increases as $0 \le w_e \le 1$, and decreases as $-1 \le w_e < 0$. An inequality constraint $|w_s| + |w_e| \le 1$ is needed to ensure that no overlap exists between the arc from s_1 to s_2 and the arc from e_1 to e_2.

Furthermore, we introduce a parameter $-1 \le w_A \le 1$ to represent the amplitude of the yaw steering acceleration component f_n:

$$f_n = \begin{cases} f w_A & \text{if } \theta \text{ is between } y_1 \text{ and } y_2 \\ -f w_A & \text{if } \theta \text{ is between } y_3 \text{ and } y_4 \\ 0 & \text{otherwise} \end{cases} \tag{6}$$

where f is the total thrust acceleration, which is computed by $f = 2\eta P/(gI_{\mathrm{sp}})$ where P is input power, I_{sp} is specific impulse, η is engine efficiency, and g is sea-level Earth gravitational acceleration. The parameter w_A is related to the yaw steering angle β by $w_A = \sin\beta$. Note that we define the inclination to increase as $0 \le w_A \le 1$, and decrease as $-1 \le w_A < 0$. The yaw steering powered arcs are applied from y_1 to y_2, and from y_3 to y_4. The determination of y_1, y_2, y_3, and y_4 is based on a parameter w_Y, which also determines the powered arc lengths between y_1 to y_2 and y_3 to y_4. The parameter w_Y is presented in [5] in detail. In addition, if the spacecraft is in the shadow (E_{en} and E_{ex} are shadow entrance and exit angles, respectively), the thrust is cut off even if it is supposed to be in a powered arc. For example, there is no thrust from y_1 to E_{ex} in the case of Fig. 1. The reason for the use of this control strategy is that the nominal trajectory generation [5] based on this control strategy is closely related to the following guidance scheme design.

Analytic Time Rates of Mean Orbital Elements Using Proposed Control Laws

The dynamics of the osculating elements [Eq. (2)] can be written in the Gauss variational form. With the assumption that the thrust is very low, we can obtain the approximate derivative of eccentric anomaly E with respect to time:

$$\frac{\mathrm{d}E}{\mathrm{d}t} \approx \frac{na}{r} \tag{7}$$

where

$$r = a(1 - e\cos E), \qquad n = \sqrt{\mu/a^3} \tag{8}$$

where μ is the gravitational parameter of the attracting body. The derivatives of osculating elements with respect to eccentric anomaly can be approximated as follows:

$$\frac{\mathrm{d}x_i}{\mathrm{d}E} = \frac{\mathrm{d}x_i}{\mathrm{d}t}\frac{\mathrm{d}t}{\mathrm{d}E} \tag{9}$$

In [5], the incremental changes in orbital elements due to low thrust per orbital revolution are derived.

$$\text{delta } x_i(f_{\text{in}}, f_{\text{out}}, [E_0, E_f], \text{“steering”}) = \int_{E_0}^{E_f} \frac{\mathrm{d}\bar{x}_i}{\mathrm{d}E}\,\mathrm{d}E \tag{10}$$

In this paper, the time rates of mean elements are readily obtained via dividing the incremental changes by the orbital period.

$$\frac{\mathrm{d}\bar{x}_i}{\mathrm{d}t}(f_{\text{in}}, f_{\text{out}}, [E_0, E_f], \text{steering}) = \left(\int_{E_0}^{E_f} \frac{\mathrm{d}x_i}{\mathrm{d}E}\,\mathrm{d}E\right) \Big/ \frac{2\pi}{n} \tag{11}$$

The expression (arg1, arg2, [arg3, arg4], arg5) in Eqs. (10) and (11) is used where “arg1” denotes in-plane acceleration amplitude, “arg2” denotes out-of-plane acceleration amplitude, “arg3” and “arg4” denote the starting and ending angles of powered arc over an revolution for integration, respectively, and “arg5” denotes the type of steering (“tangential,” “inertial” or “yaw”).

The analytic time rates of mean elements due to the tangential steering are presented in [5,19]. The elliptic integrals of the first and second kinds in Eqs. (10) and (11) for the tangential steering contain the following integrands, which can be approximated by the series expansions:

$$\sqrt{1-e^2\cos^2 E} = 1 - \frac{1}{2}e^2\cos^2 E - \frac{1}{2\cdot 4}e^4\cos^4 E - \frac{1\cdot 3}{2\cdot 4\cdot 6}e^6\cos^6 E - \ldots \tag{12}$$

$$\frac{1}{\sqrt{1-e^2\cos^2 E}} = 1 + \frac{1}{2}e^2\cos^2 E + \frac{1\cdot 3}{2\cdot 4}e^4\cos^4 E + \frac{1\cdot 3\cdot 5}{2\cdot 4\cdot 6}e^6\cos^6 E + \ldots \tag{13}$$

The integrals of Eqs. (12) and (13) with respect to E include the term $\int \cos^n E\,\mathrm{d}E$, which is computed using an iteration procedure

$$\int \cos^n E\,\mathrm{d}E = \frac{1}{n}\cos^{n-1}E\sin E + \frac{n-1}{n}\int \cos^{n-2}E\,\mathrm{d}E \tag{14}$$

where

$$\int \cos E\,\mathrm{d}E = \sin E \tag{15}$$

$$\int \cos^2 E\,\mathrm{d}E = \frac{1}{2}E + \frac{1}{4}\sin 2E \tag{16}$$

The analytic time rates of mean elements due to inertial steering and constant yaw steering are developed without approximations [5]. Therefore, the total analytic time rates of mean elements due to thrust acceleration are (using the steering in Fig. 1 as an example) as follows:

$$\begin{aligned}\frac{\mathrm{d}\bar{x}_i}{\mathrm{d}t} &= \frac{\mathrm{d}\bar{x}_i}{\mathrm{d}t}\left(0, f, [\bar{E}_{\text{ex}}, \bar{s}_1], \text{yaw}\right) \\ &+ \frac{\mathrm{d}\bar{x}_i}{\mathrm{d}t}\left(\sqrt{f^2 - f_n^2}, 0, [\bar{s}_1, \bar{y}_2], \text{tangential}\right) \\ &+ \frac{\mathrm{d}\bar{x}_i}{\mathrm{d}t}\left(0, f_n, [\bar{s}_1, \bar{y}_2], \text{yaw}\right) + \frac{\mathrm{d}\bar{x}_i}{\mathrm{d}t}\left(f, 0, [\bar{y}_2, \bar{s}_2], \text{tangential}\right) \\ &+ \frac{\mathrm{d}\bar{x}_i}{\mathrm{d}t}\left(0, f, [\bar{y}_3, \bar{e}_1], \text{yaw}\right) + \frac{\mathrm{d}\bar{x}_i}{\mathrm{d}t}\left(\sqrt{f^2 - f_n^2}, 0, [\bar{e}_1, \bar{y}_4], \text{inertial}\right) \\ &+ \frac{\mathrm{d}\bar{x}_i}{\mathrm{d}t}\left(0, f_n, [\bar{e}_1, \bar{y}_4], \text{yaw}\right) + \frac{\mathrm{d}\bar{x}_i}{\mathrm{d}t}\left(f, 0, [\bar{y}_4, \bar{e}_2], \text{inertial}\right)\end{aligned} \tag{17}$$

Moreover, the mean mass flow rate is computed as (using the steering in Fig. 1 as an example)

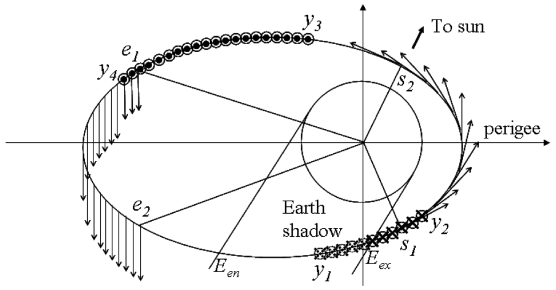

Fig. 1 Illustration of control laws (all angular variables are evaluated in true anomaly).

$$\frac{\mathrm{d}\bar{m}}{\mathrm{d}t} = -\frac{f}{gI_{\text{sp}}}\cdot\frac{1}{2\pi}\Big[(\bar{E}_{\text{ex}} - e\sin\bar{E}_{\text{ex}} - \bar{s}_2 + e\sin\bar{s}_2) + (\bar{y}_3 - e\sin\bar{y}_3 - \bar{e}_2 + e\sin\bar{e}_2)\Big] \tag{18}$$

The overbars in Eqs. (17) and (18) imply that the corresponding angular variables are evaluated in eccentric anomaly. To compute Eqs. (17) and (18), an algorithm is required for determining the sequential order of angular variables in Fig. 1 within an orbital revolution. The total time rates of mean elements are the sum of Eq. (17) and the time rates of mean elements J_2 perturbations, which can be found in many textbooks on spacecraft dynamics.

For trajectory propagation, the time interval can be set at a large time step such as one or two days, which is also used in [3,18]. The analytic solution of the sun’s direction unit vector is used for the onboard guidance to compute the Earth’s shadow exit/entrance angles [20]. The fourth-order Runge–Kutta method with fixed step size is employed to propagate the differential equation of mean orbital elements.

Guidance Scheme Design

The near-optimal transfer trajectories and open-loop guidance schemes using the proposed control strategy were described in [5]. The key idea to use the proposed control strategy is that the parameters w_s, w_e, w_A, and w_Y can be adjusted to achieve different incremental changes of semimajor axis, eccentricity, and inclination over a time horizon. The parameters w_s, w_e, w_A, and w_Y within each transfer revolution are interpolated through a number of nodes $G_{w_s}(t_n)$, $G_{w_e}(t_n)$, $G_{w_A}(t_n)$, and $G_{w_Y}(t_n)$ in terms of time, which are optimized by nonlinear optimization programming. Therefore, a nominal trajectory and control is represented by optimal solutions of states, optimal control-related parameters $G_{w_s}(t_n)$, $G_{w_e}(t_n)$, $G_{w_A}(t_n)$, and $G_{w_Y}(t_n)$, and the transfer time. Note that each of these three control laws is applied to appropriate orbital arc segments, and coast arcs may exist between powered arcs. Therefore, we expect to remove orbital element errors by changing the powered arc lengths of different steering programs. Furthermore, the modulation of variable specific impulse may be considered as an alternate option to provide a control freedom for the guidance scheme.

Nonlinear Model Predictive Control over Finite Horizons

Nonlinear model predictive control (NMPC) [21], also called receding horizon control, repeatedly computes the control input by solving an optimal control problem over a given time horizon, producing an open-loop optimal control sequence. The first control over the total time span in the sequence is applied at the initial time. At the subsequent sampling instant, a new optimal control is formulated and solved based on the new measurements. NMPC has been successfully used in many areas, such as in the process control industry. The main drawback of NMPC is the computation time of recalculating new optimal control for the real-time control system. However, this drawback is not significant for the orbital transfers in this paper which last several months.

The concept of NMPC is employed to construct the guidance scheme by tracking nominal mean elements over a finite time

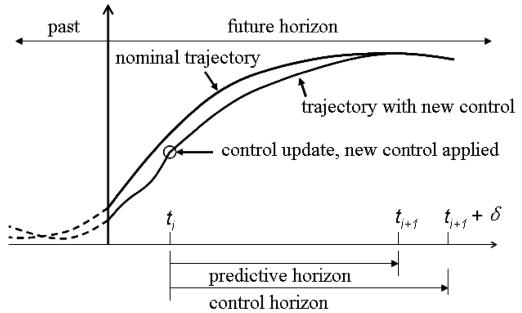

Fig. 2 Illustration of model predictive control.

horizon. Based on the results by trajectory optimization, nodes of optimal control parameters $G_{w_s}(t_n)$, $G_{w_e}(t_n)$, $G_{w_A}(t_n)$, and $G_{w_Y}(t_n)$ and mean elements along the time history are obtained. As illustrated in Fig. 2, an optimization problem over a finite time horizon for guidance can be stated as follows at a specific time constant t_i:

Find

$$\mathbf{x} = [w_s, w_e, w_A] \tag{19}$$

minimize

$$f(\mathbf{x}) = \left(\frac{[a_i + (\mathrm{d}a_i/\mathrm{d}t)\Delta t - a^*_{i+1}]}{a_i}\right)^2 + \left(e_i + \frac{\mathrm{d}e_i}{\mathrm{d}t}\Delta t - e^*_{i+1}\right)^2 + \left(i_i + \frac{\mathrm{d}i_i}{\mathrm{d}t}\Delta t - i^*_{i+1}\right)^2 \tag{20}$$

subject to

$$|w_s| + |w_e| \le 1 \tag{21}$$

Initial condition orbital elements a_i, e_i, i_i, Ω_i, ω_i at t_i (may deviate from the nominal values a^*_i, e^*_i, i^*_i, Ω^*_i, ω^*_i).

The optimization problem's goal is to find optimal parameters w_s, w_e, w_A to minimize the mean orbital element errors at t_{i+1} with the known orbital mean elements at t_i. The time intervals Δt are expressed by $t_{i+1} + \delta - t_i$ ($\delta = 0$), which is deemed a finite time horizon. The nonnegative parameter δ represents the fact that the predictive horizon may be greater than and equal to the control horizon, but, usually, these two horizons are the same. The nominal mean elements a^*_{i+1}, e^*_{i+1}, i^*_{i+1} are at t_{i+1}. The updates of parameters $\mathbf{x} = [w_s, w_e, w_A]$ results in new control laws that are used from t_i to t_{i+1} to guide the spacecraft. At the time constant t_{i+1}, the same optimization problem is formed and the same procedure is repeated until the final transfer time is reached. In the guidance scheme, w_Y is fixed and only w_A is adjusted to remove the inclination error. The value of w_Y at t_i is interpolated from the nominal nodal values of $G_{w_Y}(t_n)$. Likewise, the initial values of w_s, w_e, w_A for optimization are interpolated from the nominal nodal values of $G_{w_s}(t_n)$, $G_{w_e}(t_n)$, $G_{w_A}(t_n)$. The constrained optimization problem is converted to an unconstrained optimization problem using a penalty function

$$g(\mathbf{x}) = f(\mathbf{x}) + \max(0, |w_s| + |w_e| - 1) \tag{22}$$

where $g(\mathbf{x})$ is the cost function to be minimized. The uncertainty interval (or lower and upper bounds) of w_s, w_e, w_A are all defined as $[-1 \quad 1]$.

The nominal mean elements of transfer trajectories are tracked such that the elements a_i, e_i, i_i, Ω_i, ω_i at t_i are the mean elements. However, the orbit determination system may output the osculating orbital elements, which should be transformed to mean elements. To simplify the guidance scheme simulation in the latter section of this study, the osculating orbital elements are directly used as mean elements, and the numerical results show that this direct substitution also results in satisfactory guidance performance.

In this study, the time horizon [Δt in Eq. (20)] for finding optimal control is fixed, unlike receding horizons in many other model predictive control schemes. During each time horizon, the spacecraft is driven to the nominal trajectory as quick as possible, even though the time horizon is at the beginning of the transfer. Furthermore, we can set the time horizon Δt to be relatively short, which implies that more parameter updates will be performed during the transfer. For the short time horizon, there are only a small number of variables to be optimized for parameter updating with satisfactory solution accuracy. In general, although it appears to be somewhat conservative, the proposed scheme is robust even if orbital deviations are relatively large.

Rosenbrock's Method

The stability of minimizing the cost function in Eq. (22) is a key point for tracking guidance using NMPC. It is usually hard for us to prove that the cost function proposed in the previous section is smooth and convex. The cost function is highly nonlinear with respect to parameters $\mathbf{x} = [w_s, w_e, w_A]$ and does not have the differentiability properties in the presence of the Earth's shadow. Therefore, these types of problems are termed "nonsmooth optimizations," and they cannot be solved by the traditional optimization method involving gradient information with guaranteed stability. The minimization of Eq. (22) requires a robust convergence property, whereas the computation time is less important because of the long-duration transfer characteristic.

The Rosenbrock's algorithm [22,23] is suitable for the minimization problem proposed in this study. The initialization and steps of this algorithm are stated as follows:

Initialization: Let $\varepsilon > 0$ be a terminal value, $j = 1$, and $k = 1$. Choose $\mathbf{d}_1, \mathbf{d}_2, \ldots, \mathbf{d}_n$ as the coordinate directions of $\mathbf{x}$ where n (e.g., $n = 3$ for $\mathbf{x} = [w_s, w_e, w_A]$) is the number of variables in $\mathbf{x}$. Choose a starting point $\mathbf{x}_1$, let $\mathbf{y}_1 = \mathbf{x}_1$, and go to the main step.

Main step:

Step 1: Search λ_j to minimize the cost function $g(\mathbf{y}_j + \lambda_j \mathbf{d}_j)$, let $\mathbf{y}_{j+1} = \mathbf{y}_j + \lambda_j \mathbf{d}_j$. If $j < n$, replace j by $j + 1$, and repeat step 1. Otherwise, go to step 2.

Step 2: Let $\mathbf{x}_{k+1} = \mathbf{y}_{n+1}$. If $\|\mathbf{x}_{k+1} - \mathbf{x}_k\| < \varepsilon$, then stop with the total iteration steps k. Otherwise, let $\mathbf{y}_1 = \mathbf{x}_{k+1}$, replace k by $k + 1$, let $j = 1$, and go to step 3.

Step 3: Form a new set of linearly independent orthogonal search directions. Denote the new directions by $\mathbf{d}_1, \mathbf{d}_2, \ldots, \mathbf{d}_n$ and repeat step 1.

The new orthogonal search directions are formed using Palmer's orthogonalization procedure [24].

$$\mathbf{d}_1 = \frac{A_1}{|A_1|} \tag{23}$$

$$\mathbf{d}_k = \frac{A_k|A_{k-1}|^2 - A_{k-1}|A_k|^2}{|A_{k-1}||A_k|\sqrt{|A_{k-1}|^2 - |A_k|^2}}, \qquad k = 2, 3, \ldots, n \tag{24}$$

where

$$A_k = \sum_{i=k}^{n} \lambda_i \mathbf{d}_i, \qquad |A_k| = \sqrt{\sum_{i=k}^{n} \lambda_i^2} \qquad k = 1, 2, \ldots, n \tag{25}$$

The upper and lower bounds of λ_j (searching interval $\begin{bmatrix} \lambda_j^L & \lambda_j^U \end{bmatrix}$) are determined from boundaries of $\mathbf{x}$ and the searching direction $\mathbf{d}_j$.

$$\lambda_j^L = \min(\lambda_{j,1}^L, \lambda_{j,2}^L, \lambda_{j,3}^L, \ldots, \lambda_{j,n}^L) \tag{26}$$

$$\lambda_j^U = \max(\lambda_{j,1}^U, \lambda_{j,2}^U, \lambda_{j,3}^U, \ldots, \lambda_{j,n}^U) \tag{27}$$

where

$$\lambda_{j,i}^U = \begin{cases} (x_i^U - x_{j,i})/d_{j,i} & i = 1, 2, \ldots, n \quad \text{if } d_{j,i} > 0 \\ (x_i^L - x_{j,i})/d_{j,i} & i = 1, 2, \ldots, n \quad \text{if } d_{j,i} < 0 \\ 2x_i^U & i = 1, 2, \ldots, n \quad \text{if } d_{j,i} = 0 \end{cases}$$
$$i = 1, 2, \ldots, n \tag{28}$$

$$\lambda_{j,i}^{L} = \begin{cases} (x_i^L - x_{j,i})/d_{j,i} & i = 1,2,\ldots,n \quad \text{if } d_{j,i} > 0 \\ (x_i^U - x_{j,i})/d_{j,i} & i = 1,2,\ldots,n \quad \text{if } d_{j,i} < 0 \\ 2x_i^L & i = 1,2,\ldots,n \quad \text{if } d_{j,i} = 0 \end{cases}$$
$$i = 1,2,\ldots,n \tag{29}$$

Note that $d_{j,i}$ is the ith element of the vector $\mathbf{d}_j (j = 1,2,\ldots,n)$, $x_{j,i}$ is the ith element of the parameter vector $\mathbf{x}_j$, and x_i^U and x_i^L are upper and lower bounds of $x_{j,i}$. The search direction $\mathbf{d}_j$ at the first iteration is defined as

$$d_{j,i} = \begin{cases} 1 & i = j \\ 0 & i \neq j \end{cases} \tag{30}$$

It is apparent that $\lambda_j^U \geq 0$ and $\lambda_j^L \leq 0$. Searching λ_j to minimize $g(\mathbf{y}_j + \lambda_j \mathbf{d}_j)$ is a one-dimension line search problem. If $\lambda_j = 0$, $\mathbf{y}_j$ is not updated and remains the same. To ensure that the new value of $g(\mathbf{y}_j + \lambda_j \mathbf{d}_j)$ is less than or equal to the old one, two uncertain intervals are proposed using the golden section search method. One minimum is searched from $[\lambda_j^L \quad 0]$, and the other minimum is from $[0 \quad \lambda_j^U]$. We assume that the cost function $g(\mathbf{y}_j + \lambda_j \mathbf{d}_j)$ is convex in these two intervals, and the minimum of two optima is the new updated value of the cost function.

The formulated unconstrained optimization problem is relatively simple, with only three variables. Specifically, the design variables are all bounded and have intuitive physical meaning. Moreover, the initial values of design variables can be obtained using the solution of nominal trajectories generated by trajectory optimization.

Guidance Scheme Implementation

A guidance scheme update time interval can be prescribed. At the beginning of each time interval, the parameter optimization is performed to find w_s, w_e, w_A. With the new values of w_s, w_e, w_A, and fixed parameter w_Y, the onboard guidance can be implemented in terms of the algorithm using the osculating orbital elements, which is presented as a minimum-fuel guidance scheme in [5]. The optimization for the guidance scheme is performed onboard with a time interval of 1–2 days or longer. After the optimal parameters are obtained, the new control is applied to the next time constant. Compared with the transfer time, usually on the order of months, the onboard parameter optimization can be considered a real-time guidance scheme. More important, the derivative-free searching method is robust.

Numerical Results

Transfers from geostationary transfer orbit (GTO) and low Earth orbit (LEO) to geostationary orbit (GEO) are presented to demonstrate the effectiveness of the proposed guidance scheme. The mean orbital elements of LEO, GTO, and GEO are given in Table 1. The spacecraft parameters and transfer cases in Table 2 are cited from [3], in which two methods are used to solve minimum-time transfers. For a reference, the corresponding solutions are provided in Table 3. To simulate and investigate the proposed guidance scheme, the transfer trajectories are numerically integrated. The gravitational forces of the sun and moon, Earth's oblateness J_2 perturbations, and Earth's shadow are considered in the simulation. The position of the sun and moon are obtained using the Jet Propulsion Laboratory planetary and lunar ephemerides [25]. The initial dates of transfers are set to 01 January 2000. A fourth-order Runge–Kutta method with variable step size has been used for precise numerical integration, and the absolute and relative tolerances are set to 10^{-8}.

Table 1 Mean orbital elements of parking orbits

Orbits	a, R_e	e	i, deg	Ω, deg	ω, deg	θ, deg
LEO	1.0860	10^{-3}	28.5	0	0	0
GTO	3.8200	0.731	27	99	0	0
GEO	6.6107	10^{-4}	10^{-4}	——	——	——

Note that the precise trajectory propagation is based on osculating orbital elements and the computation of guidance parameters is performed in terms of mean orbital elements. From a theoretical viewpoint, the osculating elements should be transformed into mean elements at each time constant to update the guidance parameters. Two methods (a least-square method and an iteration method) are introduced in [18]. The transformation procedures are slightly complicated and would increase the onboard computational burden. In the simulation of this work, the transformation is not performed due to the feedback mechanism of the proposed guidance scheme. Mean elements are deemed osculating elements in the simulation, which still shows satisfactory tracking performances.

The orbital errors can be caused by many factors, like launch vehicle errors, navigation uncertainties, and thrust execution errors. Without losing generality, we assume that the initial orbital elements errors caused by whatever reasons exist at the starting time of each transfer, and the orbital deviations are expected to be corrected during the nominal transfer time without considering navigation uncertainties and thrust execution errors.

Guidance Cases for Fixed-Time Transfers with Constant Specific Impulses

Based on the solutions in Table 3, we are able to solve a series of fixed-time, fuel-saving transfers whose transfer times are greater than the minimum transfer times. For example, a 100-day GTO–GEO and a 300-day LEO–GEO transfer are solved [5]. For these two transfers, the powered arcs using three control laws are relatively short. Therefore, if the spacecraft deviates from the nominal trajectories, the guidance scheme is able to change the powered arc lengths of different steering programs to reduce orbital deviations. The nominal mean elements are given every two days for GTO–GEO transfers and one day for LEO–GEO transfers. The guidance scheme is performed onboard every two days for both transfers.

The actual initial mean orbital elements are presented in Table 4. In general, initial orbital errors of GTO are greater than the LEO's. The time histories of semimajor axis and inclination for GTO–GEO and LEO–GEO transfers, both without and with guidance, are presented in Figs. 3–6, respectively. The mean elements of nominal trajectories are also plotted accordingly. It is shown that the spacecraft continuously deviates from the nominal trajectories if no guidance is applied; with the proposed guidance, the spacecraft returns to the nominal trajectories and then keeps tracking the nominal mean elements with satisfactory performance. The thrust direction (either nominal or actual) within each revolution has the same control structure shown in Fig. 1, only with different arc lengths of each steering program. For example, the nominal values of $[w_s, w_e, w_A]$ for the first revolution of the GTO–GEO transfer are $[0.826 \quad -.0174 \quad -0.748]$, and the onboard optimization result for parameter updating gives $[0.992 \quad -0.008 \quad -0.072]$. The new parameters imply that more control weights are for the tangential steering to reduce semimajor axis errors at the beginning of the transfer.

The comparison of propellant masses for GTO–GEO nominal trajectories, unguided, and guided trajectories is shown in Table 5. For LEO–GEO transfers, the propellant masses of transfer

Table 2 Spacecraft parameters and transfer cases

Transfer case	P, kW	I_{sp}, s	η	m_0, kg	Initial thrust-to-weight ratio
GTO–GEO	5	3300	0.65	450	4.55×10^{-5}
LEO–GEO	10	3300	0.65	1200	3.41×10^{-5}

Table 3 Optimal solutions obtained in [3] (in 2000 yr)

Case	t_f, (DM) [3], (days)	t_f, (SEPSPOT) [1,3], (days)
GTO–GEO	67.0	66.6
LEO–GEO	200.3	198.8

Table 4 Actual mean orbital elements of LEO and GTO

Orbits	a, R_e	e	i, deg	Ω, deg	ω, deg	θ, deg
LEO	1.0782	0.004	29.8	1	5	0
GTO	3.6200	0.7	25.8	100	5	0

trajectories, both without and with initial element errors, are also shown in Table 5. In the presence of errors in initial mean elements, the propellant mass of guided trajectories increases by about 9% for the GTO–GEO transfer and by about 14% for the LEO–GEO transfer. For the LEO–GEO transfer even without errors in initial mean elements, the propellant mass of the guided trajectory still increases by about 4%. The spacecraft experiences a relatively long time in the Earth's shadow for the LEO–GEO transfers. This plays a more significant role to affect the propellant consumption. Note that the propellant mass differences in nominal and unguided LEO–GEO trajectories without initial orbital errors are primarily due to the orbital averaging approximation, sun's gravitational force, and lunar gravitational force.

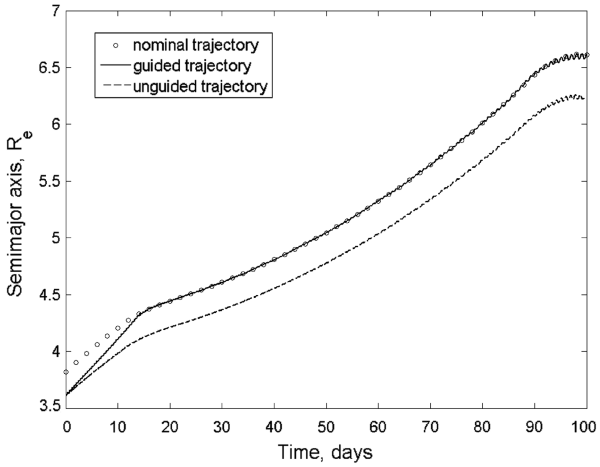

Fig. 3 Time histories of semimajor axis (100-day GTO–GEO transfers).

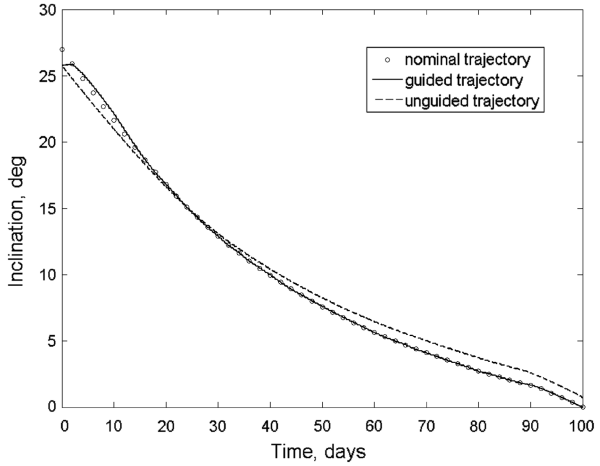

Fig. 4 Time histories of inclination (100-day GTO–GEO transfers).

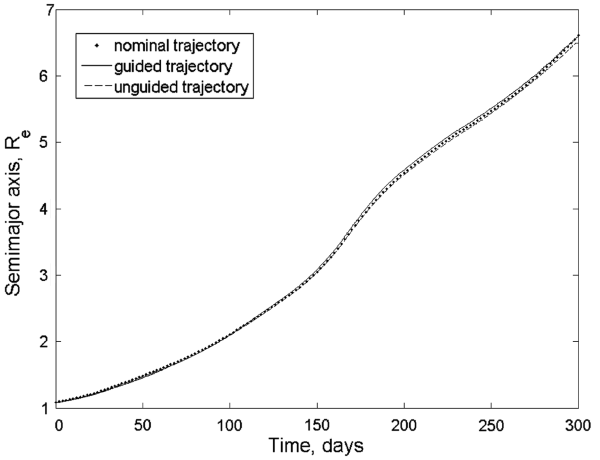

Fig. 5 Time histories of semimajor axis (300-day LEO–GEO transfers).

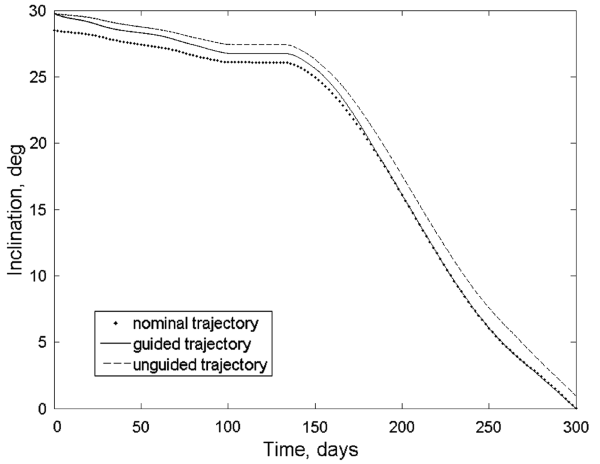

Fig. 6 Time histories of inclination (300-day LEO–GEO transfers).

Guidance Cases for Fixed-Time Transfers with Variable Specific Impulse

In the previous section, it is demonstrated that the guidance scheme is implemented only by changing the powered arc lengths of different steering programs. If the transfer time is close to the minimum solution, the coasting arcs between powered arcs are relatively short. For example, we can solve a 74-day GTO–GEO transfer using the approach in [5]. In this case, to satisfactorily track mean elements, a viable means is to have the specific impulse modulated, which eventually changes the thrust magnitude. In this paper, the specific impulse is simply modeled as $I_{\text{sp}} = I^*_{\text{sp}} + 300a_{\text{sp}}$ s (the parameter 300 s can be changed to other values for constraint on I_{sp}), and then the constraint on the total impulse is defined within the 74-day transfer. I^*_{sp} is the nominal value and a_{sp} is a parameter between -1 and 1, which is the same as the upper and lower bounds of parameters w_s, w_e, w_A. The parameter a_{sp} is then an additional optimization variable so that the search vector space is $\mathbf{x} = [w_s, w_e, w_A, a_{\text{sp}}]$. The initial value of $a_{\text{sp}} = 0$ is the constant value in the nominal trajectories.

Table 5 Propellant masses of GTO–GEO transfers with initial errors

Transfer	Nominal (orbital averaging)	Unguided (precise integration)	Guided (precise integration)
GTO–GEO	30.30 kg	30.94 kg	33.14 kg
LEO–GEO, with error	182.47 kg	185.28 kg	208.02 kg
LEO–GEO, no error	182.47 kg	183.80 kg	190.00 kg

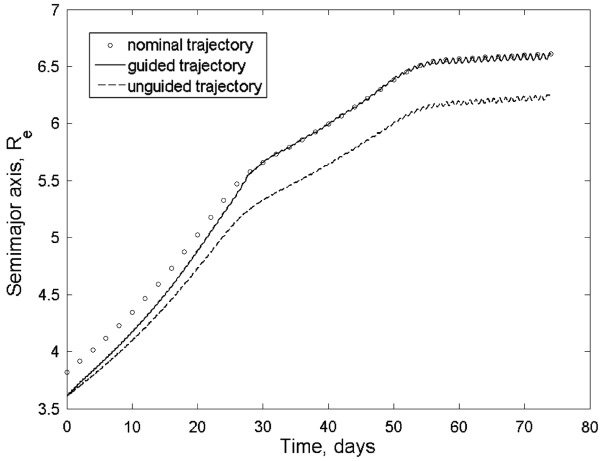

Fig. 7 Time histories of semimajor axis (74-day GTO–GEO transfers).

The GTO–GEO transfer with errors in initial mean elements (same corresponding case in Table 4) is simulated including modulation of specific impulse. The propellant masses for the simulation results of 74-day GTO–GEO transfers with variable I_{sp} are as follows: nominal (orbital averaging) is 34.26 kg, unguided (precise integration) is 34.30 kg, and guided (precise integration) is 38.17 kg. The propellant mass of guided trajectories increases by about 11%. In Figs. 7 and 8, the semimajor axis and inclination for nominal, unguided, and guided trajectories are presented. Note that the specific impulse remains constant within two days, which is the time interval to update guidance parameters. The time history of specific impulse is presented in Fig. 9. The I_{sp} has been at its lower bound for more than 20 days, which means that the thrust magnitude is greater than the nominal value during this phase.

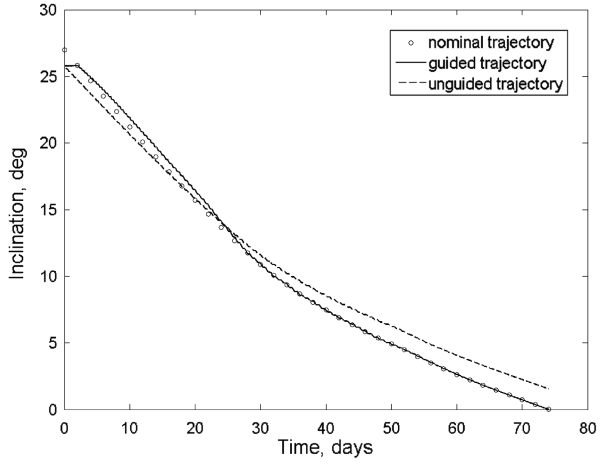

Fig. 8 Time histories of inclination (74-day GTO–GEO transfers).

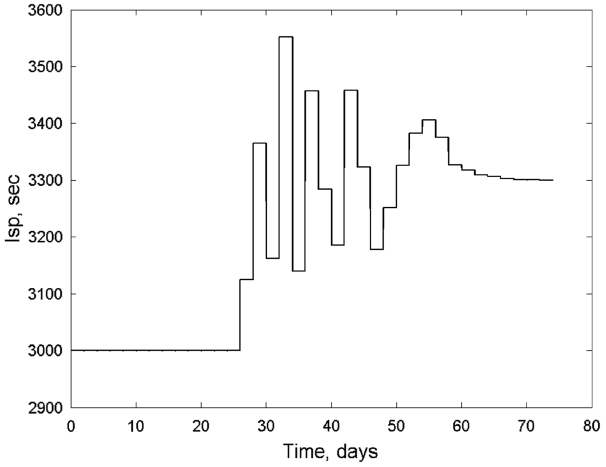

Fig. 9 Time histories of variable specific impulse (74-day GTO–GEO guided transfer).

Table 6 Maximum times of iterations and cost function evaluations

Transfer	Number of variables	Max. iteration steps	Max. no. of evaluations
GTO–GEO	3	20	2169
LEO–GEO, with error	3	23	2104
LEO–GEO, no error	3	21	2324
GTO–GEO, variable I_{sp}	4	10	1535

Computational Load

The computation load of each parameter update is an issue to be clarified. According to Rosenbrock's method presented in this study, each optimum searching iteration contains a number of line searches for three or four variables. The computational load (or speed) can be represented by the numbers of cost function evaluations for each update. Note that the updating time interval is two days, such that there are 50 and 150 parameter updates for the 100-day GTO–GEO and 300-day LEO–GEO transfers, respectively. The maximum iteration step of Rosenbrock's method among all updates is recorded in Table 6 for four simulation cases with the terminal value ε set to 10^{-3}.

Each iteration of Rosenbrock's method contains two line searches for two uncertain intervals [see Eqs. (26–29) and the texts that follow]. The smallest numbers of function evaluations n using the golden section method satisfies $0.618^{n-1} \geq 10^{-4}/\Delta$ where Δ is the uncertainty interval of the line search and 10^{-4} is the final interval of uncertainty. For each simulation case, the maximum numbers of the cost function evaluations among all updates are also obtained in Table 6. In terms of the maximum number, the approximate computational speed can be estimated for a specific onboard processor.

Conclusions

An autonomous nonlinear guidance scheme for low-thrust Earth-orbit spacecraft has been presented. The construction of the guidance scheme is based on trajectory tracking using model predictive control over finite time horizons. A control strategy including three simple control laws is used to track nominal mean elements. Changing the powered arc length of each control law is a novel characteristic among existing guidance schemes. The onboard tracking control optimization, performed by the Rosenbrock's method without calculating derivatives, guarantees the robustness of optimum searching. The numerical simulation results show that the guidance scheme successfully corrects orbital deviations and finally drives the spacecraft to the target orbit within the nominal transfer time. The propellant masses of guided trajectories increase by about 9–14% in the various scenarios. Finally, the computational load has been presented. Compared with other tracking algorithms and Lyapunov-based guidance, the proposed scheme considers a coasting mechanism, specific impulse modulation, and the effects of the Earth's oblateness and shadowing. In summary, the guidance scheme is a suitable candidate for realistic low-thrust missions.

There are still some open questions left in the framework of this study. Maybe there exist other elegant and concise control strategies for trajectory tracking. Singularity exists due to the use of classical orbital elements, and so nonsingular orbital elements are expected to construct control laws. The online robust nonlinear optimization method is also a topic for the application in this paper. In addition, any other parameters related to minimizing the orbital elements errors between predictive and nominal trajectories could be included.

Acknowledgments

This work has been supported by the National Natural Science Foundation of China (Grant No. 10603005) and Academy of Opto-Electronics (Grant No. AOE-CX-200601).

References

[1] Sackett, L. L., Malchow, H. L., and Edelbaum, T. N., "Solar Electric Geocentric Transfer with Attitude Constraints: Analysis," NASA, CR-134927, Aug. 1975.

[2] Geffroy, S., and Epenoy, R.,"Optimal Low-Thrust Transfers with Constraints: Generalization of Averaging," *Acta Astronautica*, Vol. 41, No. 3, 1997, pp. 133–149. doi:10.1016/S0094-5765(97)00208-7

[3] Kluever, C. A., and Oleson, S. R., "Direct Approach for Computing Near-Optimal Low-Thrust Earth-Orbit Transfers," *Journal of Spacecraft and Rockets*, Vol. 35, No. 4, 1998, pp. 509–515.

[4] Ferrier, C., and Epenoy, R., "Optimal Control for Engines with Electro-Ionic Propulsion Under Constraint of Eclipse," *Acta Astronautica*, Vol. 48, No. 4, 2001, pp. 181–192. doi:10.1016/S0094-5765(00)00158-2

[5] Gao, Y., "Near-Optimal Very Low-Thrust Earth-Orbit Transfers and Guidance Schemes," *Journal of Guidance, Control, and Dynamics*, Vol. 30, No. 2, 2007, pp. 529–539. doi:10.2514/1.24836

[6] Kugelberg, J., Bodin, P., Persson, S., and Rathsman, P., "Accommodating Electric Propulsion on SMART-1," *Acta Astronautica*, Vol. 55, No. 2, 2004, pp. 121–130. doi:10.1016/j.actaastro.2004.04.003

[7] Rathsman, P., Kugelberg, J., Bodin, P., Racca, G. D., Foing, B., and Stagnaro, L., "SMART-1: Development and Lessons Learnt," *Acta Astronautica*, Vol. 57, Nos. 2–8, 2005, pp. 455–468. doi:10.1016/j.actaastro.2005.03.041

[8] Gil-Fernandez, J., Graziano, M., Gomez-Tierno1, M. A., and Millic, E., "Autonomous Low-Thrust Guidance: Application to SMART-1 and BepiColombo," *Annals of the New York Academy of Sciences*, Vol. 1017, Astrodynamics, Space Missions, and Chaos, New York Academy of Sciences, New York, 2004, pp. 307–327.

[9] Kluever, C. A., "Simple Guidance Scheme for Low-Thrust Orbit Transfers," *Journal of Guidance, Control, and Dynamics*, Vol. 21, No. 6, 1998, pp. 1015–1017.

[10] Kluever, C. A., "Low-Thrust Orbit Transfer Guidance Using an Inverse Dynamics Approach," *Journal of Guidance, Control, and Dynamics*, Vol. 18, No. 1, 1995, pp. 187–189.

[11] Kluever, C. A., and Shaughnessy, D. J., "Trajectory-Tracking Guidance Law for Low-Thrust Earth-Orbit Transfers," *Journal of Guidance, Control, and Dynamics*, Vol. 23, No. 4, 2000, pp. 754–756.

[12] Ilgen, M. R., "Low Thrust OTV Guidance Using Lyapunov Optimal Feedback Control Techniques," *AAS/AIAA Astrodynamics Specialist Conference*, American Astronautical Society Paper 93-680, Aug. 1993.

[13] Chang, D. E., Chichka, D. F., and Marsden, J. E., "Lyapunov-Based Transfer Between Elliptic Keplerain Orbits," *Discrete and Continuous Dynamical Systems, Series B*, Vol. 2, No. 1, 2002, pp. 57–67.

[14] Gurfill, P., "Nonlinear Feedback Control of Low-Thrust Orbital Transfer in a Central Gravitational Field," *Acta Astronautica*, Vol. 60, Nos. 8–9, 2007, pp. 631–648. doi:10.1016/j.actaastro.2006.10.001

[15] Petropoulos, A. E., "Low-Thrust Orbit Transfers Using Candidate Lyapunov Functions with a Mechanism for Coasting," *AIAA/AAS Astrodynamics Specialist Conference*, AIAA Paper 2004-5089, Aug. 2004.

[16] Arrieta-Camacho, J. J., and Biegler, L. T., "Real Time Optimal Guidance of Low-Thrust Spacecraft: An Application of Nonlinear Model Predictive Control," *Annals of the New York Academy of Sciences*, Vol. 1065, New Trends in Astrodynamics and Applications, New York Academy of Sciences, New York, 2005, pp. 174–188.

[17] Cefola, P. J., Long, A. C., and Holloway, G., Jr., "Long-Term Prediction of Artificial Satellite Orbits," *AIAA 12th Aerospace Sciences Meeting*, AIAA Paper 74-170, Jan. 1974.

[18] Danielson, D. A., Sagovac, C. P., Neta, B., and Early, L. W., "Semi-Analytic Satellite Theory," U.S. Naval Postgraduate School, TR NPS-MA-95-002, 1995.

[19] Gao, Y., and Kluever, C. A., "Analytic Orbital Averaging Technique for Computing Tangential-Thrust Trajectories," *Journal of Guidance, Control, and Dynamics*, Vol. 28, No. 6, 2005, pp. 1320–1323. doi:10.2514/1.14698

[20] Vallado, D. A., *Fundamentals of Astrodynamics and Applications*, Kluwer Academic, Norwell, MA, 2001, pp. 263–267.

[21] Allgower, F., and Zheng, A. (eds.), *Nonlinear Model Predictive Control*, Vol. 26, Progress in Systems and Control Theory, Birkhauser Basel, Boston, 2000.

[22] Rosenbrock, H. H., "Automatic Method for Finding the Greatest or Least Values of a Function," *Computer Journal*, Vol. 3, No. 3, 1960, pp. 175–184. doi:10.1093/comjnl/3.3.175

[23] Bazaraa, M. S., Sherali, H. D., and Shetty, C. M., *Nonlinear Programming Theory and Algorithm*, Wiley, New York, 1993, pp. 291–300.

[24] Palmer, J. R., "Improved Procedure for Orthogonalising the Search Vectors in Rosenbrock's and Swann's Direct Search Optimization Methods," *Computer Journal*, Vol. 12, No. 1, 1969, pp. 69–71.

[25] Standish, E. M., "JPL Planetary and Lunar Ephemerides DE402/LE402," *Bulletin of the American Astronomical Society*, Vol. 27, June 1995, p. 1203.